DYNAMICS OF LOCALLY ROTATIONALLY SYMMETRIC BIANCHI TYPE VIII COSMOLOGIES WITH ANISOTROPIC MATTER

Gernot HEIßEL

Abstract. This paper is a study of the effects of anisotropic matter sources on the qualitative evolution of spatially homogenous cosmologies of Bianchi type VIII. The analysis is based on a dynamical system approach and makes use of an anisotropic matter family developed by Calogero and Heinzle which generalises perfect fluids and provides a measure of deviation from isotropy. Thereby the role of perfect fluid solutions is put into a broader context.

The results of this paper concern the past and future asymptotic dynamics of locally rotationally symmetric solutions of type VIII with anisotropic matter. It is shown that solutions whose matter source is sufficiently close to being isotropic exhibit the same qualitative dynamics as perfect fluid solutions. However a high degree of anisotropy of the matter model can cause dynamics to differ significantly from the vacuum and perfect fluid case.

1. Introduction and motivation

For spatially homogenous (SH) spacetimes the Einstein-matter equations for a large variety of matter sources reduce to an autonomous system of ordinary differential equations in time. Thus the mathematical theory of dynamical systems can be applied to gain insights into the qualitative behaviour of SH solutions. This approach has been used in mathematical cosmology, e.g. to address questions relevant for observational cosmology, in particular concerning the role the Friedmann solutions play in the more general context of SH cosmologies that are not spatially isotropic in general. On the other hand the interest in SH models is nourished by the believe that the dynamics of SH cosmologies towards the initial singularity is crucial for the understanding of the behaviour of more general spacetimes close to singularities; cf. [1] and references therein.

Less is known about SH solutions with matter sources more general than perfect fluids. Calogero and Heinzle have developed a matter family naturally generalising perfect fluids that contains large classes of anisotropic matter sources and is suited for a dynamical system analysis. It includes a measure of the deviation from isotropy and thus allows to investigate the role of perfect fluid solutions in the more general context of solutions with anisotropic matter. The SH cosmologies considered were of Bianchi type I, and locally rotationally symmetric (LRS) types I, II and IX; cf. [2, 3]. While dynamical system analyses with specific anisotropic matter sources have been carried out before, the approach by Calogero and Heinzle can be regarded as a first step towards a systematic study of the effects of anisotropic matter to the qualitative dynamics of SH cosmologies.

This paper is concerned with the analysis of SH cosmologies of LRS Bianchi type VIII with anisotropic matter. In section 2 the basic features of the anisotropic matter family are stated, and the state space and evolution equations for LRS type VIII are given. The dynamical system analysis is performed in section 3, where

Date: February 26, 2013.
PACS: 98.80.Jk, 04.20.DW.

some technical details on the analysis of the flow at infinity are contained in the appendix. The results are given and discussed in section 4, where the main result is formulated in theorem 1 and corollaries 1 and 2. As a small byproduct, the results cover the future asymptotics for perfect fluids with $p = w\rho$ and $w \in \left(-\frac{1}{3}, 0\right)$, which might fill a little gap in the literature. Section 5 is concerned with an extension of the formalism to treat Vlasov matter dynamics with massive particles.

Part of the material needed in sections 2, 3 and 5 has already been presented in [3] or [4] to analyse LRS Bianchi types I, II and IX. At these points in the text, only the crucial steps and results are quoted from there.

2. The LRS Bianchi type VIII setup

In a frame $(\mathrm{d}t, \hat{\omega}^1, \hat{\omega}^2, \hat{\omega}^3)$ adapted to the symmetries, an LRS Bianchi class A metric has the form

$$^4g = -\,\mathrm{d}t \otimes \mathrm{d}t + g_{11}(t)\,\hat{\omega}^1 \otimes \hat{\omega}^1 + g_{22}(t)\,(\hat{\omega}^2 \otimes \hat{\omega}^2 + \hat{\omega}^3 \otimes \hat{\omega}^3).$$

In type VIII, $\mathrm{d}\hat{\omega}^i = -\frac{1}{2}\epsilon_{jkl}\hat{n}^{ij}\hat{\omega}^k \wedge \hat{\omega}^l$, with $[\hat{n}^{ij}] \equiv \mathrm{diag}(-1, 1, 1)$. Greek indices denote spacetime components while Latin indices label spatial components w.r.t. the adapted frame. The metric will be subject to the Einstein equations—without cosmological constant—in geometrised units ($8\pi G = c = 1$), cf. [3, Eq 2].

2.1. **The anisotropic matter family.** For a perfect fluid that is non-tilted with respect to $\mathrm{d}t$, the components of the stress-energy tensor are $[T^\mu{}_\nu] = \mathrm{diag}(\rho, p, p, p)$, where ρ and p denote the energy density and pressure of the fluid. It is an isotropic matter model since the eigenvalues of $[T^i{}_j]$ are all equal. When $p = w\rho$ with $w = \mathrm{const}$, the fluid is said to obey a linear equation of state.[1]

The matter models considered in this paper form a family of models generalising perfect fluids with linear equation of state. This family of models is described in detail in [3, section 3]. In the following, a brief description tailored to the present purposes is given:

The components of the stress-energy tensor are $[T^\mu{}_\nu] = \mathrm{diag}(\rho, p_1, p_2, p_2)$ where the energy density $\rho \geq 0$ and the isotropic pressure $p := \sum_i p_i/3$ obey a linear equation of state $p = w\rho$, with $w = \mathrm{const}$. Defining the dimensionless rescaled principal pressures as $w_i := p_i/\rho$ it is clear that $w = \sum_i w_i/3$, which in turn implies that w_1 and w_2 are not independent once w is given. As a consequence of the Einstein equations and some basic assumptions on the matter family given in [3, section 3], w_2 (and thus w_1) is a function of the quantity $s := \frac{g^{22}}{\sum_i g^{ii}} \in \left(0, \frac{1}{2}\right)$. Clearly, s gives a measure of anisotropy of the spatial metric components while w_2 encodes the anisotropy of the matter content.[2] The simple example of isotropic matter corresponds to $w_1 = w_2 = w$. Also, note that $s \to 0$ and $s \to \frac{1}{2}$ correspond to $g_{22} \to \infty$ (or $g_{11} \to 0$) and $g_{11} \to \infty$ (or $g_{22} \to 0$) respectively, i.e. to a singular metric. A basic assumption is that the limit of w_1 for $s \to \frac{1}{2}$ coincides with the limit of w_2 for $s \to 0$, i.e. that $w_1\left(\frac{1}{2}\right) = w_2(0)$. Hence one can define an anisotropy parameter

$$\beta := 2\frac{w - w_2(0)}{1 - w} \tag{1}$$

that provides a measure of deviation from an isotropic matter state in the extremal cases where the metric is singular. Note that $\beta = 0$ corresponds to matter models that behave like a perfect fluid close to singularities.

The analysis in section 3 will show that the qualitative dynamics of LRS Bianchi type VIII solutions does not depend on the whole function w_2 but merely on the

[1] For example, $w = 0$ corresponds to dust and $w = \frac{1}{3}$ to radiation.

[2] In [3] $w_2(s)$ is called anisotropy function and denoted by $u(s)$.

value $w_2(0)$ where the metric is singular. Thus any two matter models of the anisotropic matter family that share the same parameters w and β also share the same qualitative dynamics, even if they have different functions $w_i(s)$. Accordingly, β serves as the parameter to investigate the influence of the anisotropy of the matter on the dynamics, even though it gives a precise measure of the anisotropy only close to singularities. Therefore, in the context of the qualitative analysis of the dynamics of solution that follows, a specific class of matter models is simply characterised by a pair (w, β) in the parameter space

$$\mathbb{P} := \left(-\tfrac{1}{3}, 1\right) \times \mathbb{R}.$$

Here w is restricted to $\left(-\frac{1}{3}, 1\right)$ since the primary interest is in matter models that obey the standard energy conditions [5, p 218–220]: The weak energy condition corresponds to $w_i \geq -1$. The strong energy condition requires the weak energy condition to hold and $w \geq -\frac{1}{3}$. The dominant energy condition is $|w_i| \leq 1$. Therefore, by (1), for the energy conditions to hold, one has to restrict β to $\left[\max\left(-2, -\frac{1+w}{1-w}\right), 1\right]$; cf. [3, table 2 in section 3.4]. The dominant energy condition is only marginally satisfied when $\beta(w)$ takes the boundary values. The parameter space $\mathbb{P}$ and the subset for which the energy conditions are satisfied is illustrated in figure 3 together with the bifurcation lines which will be explained in section 3.

2.2. **The Einstein equations as a dynamical system.** LRS Bianchi types VIII and IX share the same evolution equations which have been derived in detail in [3]. This subsection gives a brief outline:

Due to spatial homogeneity, the Einstein equations for LRS type VIII with the above matter source are a constrained autonomous system of ordinary differential equations in t for the components of the spatial metric g_{ij} and the extrinsic curvature k_{ij}. This system is then written in terms of quantities that are standard cosmological parameters and/or bring the equations into suitable shape. These quantities are the Hubble scalar $H := -\frac{1}{3}({k^1}_1 + 2{k^2}_2)$, the shear variable $\sigma_+ := \frac{1}{3}({k^1}_1 - {k^2}_2)$ and the quantity $m_1 := \sqrt{g_{11}}/g_{22}$. Finally these are divided by the dominant variable $D := \sqrt{H^2 - 1/(3g_{22})} > 0$ to obtain the normalised variables $(H_D, \Sigma_+, M_1) := (H, \sigma_+, m_1)/D$.[3]

The resulting representation of the Einstein equations for anisotropic matter filled LRS Bianchi type VIII spacetimes is then given by the dynamical system

$$\begin{bmatrix} H_D \\ \Sigma_+ \\ M_1 \end{bmatrix}' = \begin{bmatrix} -(1-H_D^2)(q - H_D\Sigma_+) \\ -(2-q)H_D\Sigma_+ - (1-H_D^2)(1-\Sigma_+^2) + \frac{M_1^2}{3} + 3\Omega\,(w_2(s) - w) \\ M_1\left(qH_D - 4\Sigma_+ + (1-H_D^2)\Sigma_+\right) \end{bmatrix} \tag{2}$$

which represents the evolution equations, and the constraints

$$\Omega + \Sigma_+^2 + \frac{M_1^2}{12} = 1 \quad \text{and} \quad 1 - H_D^2 = -\frac{1}{3D^2 g_{22}} < 0. \tag{3}$$

The former is the Hamiltonian constraint, while the latter follows directly from the definition of D. $\Omega := \frac{\rho}{3D^2} > 0$ denotes the normalised energy density and $q := 2\Sigma_+^2 + \frac{1+3w}{2}\Omega$ the deceleration parameter. The prime denotes derivatives with respect to rescaled time; $(\cdot)' := \frac{1}{D}\frac{\partial}{\partial t}(\cdot)$. Note that the definition of M_1 and the second constraint imply that s can be regarded as a function of H_D and M_1, $s = \left(2 - 3\frac{1-H_D^2}{M_1^2}\right)^{-1}$. Therefore (2) is a closed system once $w_2(s)$ is prescribed through the 'equation of state' of the anisotropic matter.

[3] In [3] this normalisation has been taken in lieu of the Hubble normalisation [6, section 5.2] mainly because it yields a compact LRS type IX state space. Although this is not the case for LRS type VIII, the dominant normalisation still has favourable properties. For example the type III form of flat spacetime is a fixed point solution in this formulation; cf. table 1.

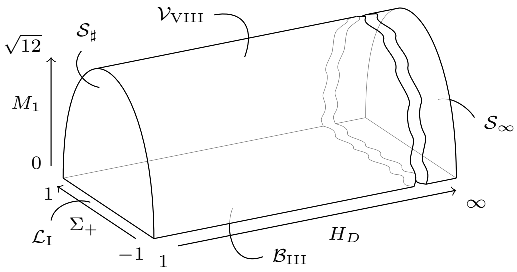

FIGURE 1. The state space $\mathcal{X}_{\mathrm{VIII}}$ and its boundary subsets.

2.3. **The state space $\mathcal{X}_{\mathrm{VIII}}$.** The LRS type VIII state space is determined by the constraints (3): Since $\Omega > 0$ and $M_1 > 0$ by definition, it follows from the Hamiltonian constraint that $\Sigma_+^2 < 1$ and $\Sigma_+^2 + \frac{M_1^2}{12} < 1$. The inequality $1 - H_D^2 < 0$ imposed by the second constraint implies that the state space is the union of two disjoint sets: $H_D > 1$ corresponds to positive H and hence to forever expanding universes, while $H_D < -1$ corresponds to forever contracting universes. However, since (2) is invariant under the reflection $(t, H_D, \Sigma_+) \to -(t, H_D, \Sigma_+)$ it suffices to restrict to the expanding case. Accordingly the LRS Bianchi type VIII state space is defined as

$$\mathcal{X}_{\mathrm{VIII}} := \left\{ \begin{bmatrix} H_D \\ \Sigma_+ \\ M_1 \end{bmatrix} \in \mathbb{R}^3 \middle| H_D \in (1,\infty), \Sigma_+ \in (-1,1), M_1 \in (0, \sqrt{12(1-\Sigma_+^2)}) \right\},$$

which forms the tunnel-like structure depicted in figure 1. The boundary subsets of $\mathcal{X}_{\mathrm{VIII}}$ are $\mathcal{V}_{\mathrm{VIII}}$, $\mathcal{B}_{\mathrm{III}}$ and $\mathcal{S}_\sharp$, which correspond to $\Omega = 0$, $M_1 = 0$ and $H_D = 1$, respectively. LRS type VIII vacuum solutions thus lie in $\mathcal{V}_{\mathrm{VIII}}$ while solutions in $\mathcal{S}_\sharp$ and $\mathcal{B}_{\mathrm{III}}$ are of Bianchi types II and III respectively; cf. [3, sections 9.2 and the first remark in 10.1]. $\mathcal{S}_\infty$, which corresponds to $H_D \to \infty$, is of course not a boundary, but one can think of it as boundary in a compactified version of the state space; cf. appendix A.

In this formulation LRS type IX cosmologies are subject to the same evolution equations (2). However there is a sign change in the second constraint of (3) leading to a different state space $\mathcal{X}_{\mathrm{IX}}$ for which $H_D \in (-1, 1)$. Figuratively speaking $\mathcal{X}_{\mathrm{IX}}$ builds the tunnel connecting $\mathcal{X}_{\mathrm{VIII}}$ with the second disjoint LRS type VIII set. Hence both $\mathcal{X}_{\mathrm{VIII}}$ and $\mathcal{X}_{\mathrm{IX}}$ share the boundary $\mathcal{S}_\sharp$. Cf. [3, section 9].

There are two challenges in connection with the analysis of the dynamical system (2) in $\mathcal{X}_{\mathrm{VIII}}$. First, $\mathcal{X}_{\mathrm{VIII}}$ is not compact. Hence one has to perform a careful analysis of the 'flow at infinity'. In the present case it will be shown that there do not exist orbits that emanate from or escape to infinity. Second, the dynamical system (2) does not extend to the line $\mathcal{L}_{\mathrm{I}}$ in $\partial\mathcal{X}_{\mathrm{VIII}}$ for that $H_D = 1$ and $M_1 = 0$ since $s(H_D, M_1)$ has no limit when $\mathcal{L}_{\mathrm{I}}$ is approached from $\mathcal{X}_{\mathrm{VIII}}$.[4] The analogous problem occurs in the context of LRS type IX, where it was overcome by introducing another set of coordinates that give regular access to this part of the boundary by 'blowing up' $\mathcal{L}_{\mathrm{I}}$; cf. [3, section 10.2]. This method can be adapted to the LRS type VIII case by applying the same coordinate transformation. However the corresponding state space is again different:

2.4. **The state space $\mathcal{Y}_{\mathrm{VIII}}$.** The coordinate transformation used to analyse $\mathcal{L}_{\mathrm{I}}$ is

$$1 - H_D^2 = 2r\cos\theta, \quad M_1^2 = 3r\sin\theta, \quad \Sigma_+ \text{ unchanged,} \tag{4}$$

[4]However $s(H_D, M_1)$ has limits when $\mathcal{L}_{\mathrm{I}}$ is approached from $\mathcal{B}_{\mathrm{III}}$ or $\mathcal{S}_\sharp$; cf. sections 3.2 and 3.3.

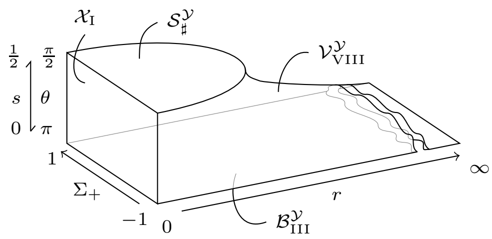

FIGURE 2. The state space $\mathcal{Y}_{\mathrm{VIII}}$ and its boundary subsets.

where $r \geq 0$ and $\theta \in [\frac{\pi}{2}, \pi]$. Thereby, $\mathcal{X}_{\mathrm{VIII}}$ is transformed to the state space

$$\mathcal{Y}_{\mathrm{VIII}} := \left\{ \begin{bmatrix} r \\ \theta \\ \Sigma_+ \end{bmatrix} \in \mathbb{R}^3 \middle| r \in \left(0, \frac{4(1-\Sigma_+^2)}{\sin\theta}\right), \theta \in \left(\frac{\pi}{2}, \pi\right), \Sigma_+ \in (-1, 1) \right\}$$

which is depicted in figure 2. From (4) one has the following correspondences between subsets of $\overline{\mathcal{X}}_{\mathrm{VIII}}$ and $\overline{\mathcal{Y}}_{\mathrm{VIII}}$:

$$\text{(5)}\quad \mathcal{X}_{\mathrm{VIII}} \sim \mathcal{Y}_{\mathrm{VIII}}, \quad \overline{\mathcal{V}}_{\mathrm{VIII}} \sim \overline{\mathcal{V}}^{\mathcal{Y}}_{\mathrm{VIII}}, \quad \overline{\mathcal{B}}_{\mathrm{III}} \sim \overline{\mathcal{B}}^{\mathcal{Y}}_{\mathrm{III}} \cup \overline{\mathcal{X}}_I, \quad \overline{\mathcal{S}}_{\sharp} \sim \overline{\mathcal{S}}^{\mathcal{Y}}_{\sharp} \cup \overline{\mathcal{X}}_I, \quad \overline{\mathcal{L}}_{\mathrm{I}} \sim \overline{\mathcal{X}}_{\mathrm{I}}.$$

$\mathcal{S}_\infty$ corresponds to a line at infinity in the context of $\mathcal{Y}_{\mathrm{VIII}}$. Furthermore, (4) defines a diffeomorphism between $\overline{\mathcal{X}}_{\mathrm{VIII}} \backslash \overline{\mathcal{L}}_{\mathrm{I}}$ and $\overline{\mathcal{Y}}_{\mathrm{VIII}} \backslash \overline{\mathcal{X}}_{\mathrm{I}}$, from which it follows that the flows in these sets are topologically equivalent. In particular,

$$\text{(6)}\qquad \mathcal{X}_{\mathrm{VIII}} \cong \mathcal{Y}_{\mathrm{VIII}}, \quad \mathcal{V}_{\mathrm{VIII}} \cong \mathcal{V}^{\mathcal{Y}}_{\mathrm{VIII}}, \quad \mathcal{B}_{\mathrm{III}} \cong \mathcal{B}^{\mathcal{Y}}_{\mathrm{III}} \quad \text{and} \quad \mathcal{S}_{\sharp} \cong \mathcal{S}^{\mathcal{Y}}_{\sharp}.$$

In contrast, the coordinate transformation performs a blowup of the line $\mathcal{L}_{\mathrm{I}}$ to the two-dimensional set $\mathcal{X}_{\mathrm{I}}$ defined by setting $r = 0$. It can be identified with the LRS Bianchi type I state space; cf. [3, section 10.2]. With (4), s can be regarded as a function of θ alone. Therefore s has a limit as $r \to 0$, which implies that the dynamical system, when expressed in the coordinates (r, θ, Σ_+), extends regularly to $\mathcal{X}_{\mathrm{I}}$.

Finally, note that since $s(\theta)$ is a bijection on $[\frac{\pi}{2}, \pi]$ one can as well choose s as coordinate instead of θ; hence the two labels on the axis in figure 2.

3. The dynamical system analysis

Whenever possible the analysis is carried out in the coordinates (H_D, Σ_+, M_1), which is in all sets except $\mathcal{X}_{\mathrm{I}}$. However the final results presented in section 4 have to be interpreted in the context of the state space $\mathcal{Y}_{\mathrm{VIII}}$ since the system (2) is not regular in $\overline{\mathcal{X}}_{\mathrm{VIII}}$, which prevents a complete global analysis in the original state space.

Since the matter parameters w and β enter the evolution equations everywhere except in the vacuum boundary and at infinity, cf. sections 3.1 and 3.5, their values determine the qualitative properties of the flow. For instance there are fixed points that only occur in the state space iff (w, β) is in a certain subset of $\mathbb{P}$. Similarly, fixed points may have different local stability properties depending on (w, β). The curves $\beta(w) \in \mathbb{P}$ dividing $\mathbb{P}$ into these subsets corresponding to qualitatively different dynamics shall be called bifurcation lines. These bifurcation lines will be found in the subsequent subsections and are plotted in figure 3.

3.1. Analysis in $\overline{\mathcal{V}}_{\mathrm{VIII}}$.

The dynamical system in $\overline{\mathcal{V}}_{\mathrm{VIII}}$ is obtained by setting $\Omega = 0$ in (2) and using (3):

$$\text{(7)}\qquad \begin{bmatrix} H_D \\ \Sigma_+ \end{bmatrix}' = \begin{bmatrix} (1-H_D^2)(H_D - 2\Sigma_+)\Sigma_+ \\ (1-\Sigma_+^2)\left(2 + (1-\Sigma_+^2) + (H_D - \Sigma_+)^2\right) \end{bmatrix}$$

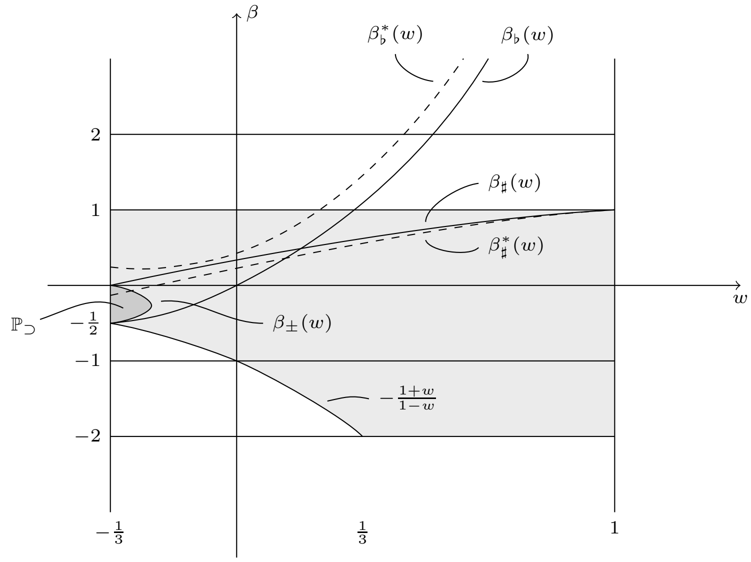

FIGURE 3. The bifurcation diagram in the parameter space $\mathbb{P}$. The shaded region (including $\mathbb{P}_\supset$) marks the subset for which the energy conditions are satisfied.

There are three fixed points in $\overline{\mathcal{V}}_{\mathrm{VIII}}$, $T := [1, -1]^{\mathrm{T}}$, $Q := [1, 1]^{\mathrm{T}}$ and $D := [2, 1]^{\mathrm{T}}$. The eigenvectors and eigenvalues of the linearisation of (7) at the fixed points determine their local stability properties. One finds[5]

$$T : \begin{bmatrix} 6 \\ 12 \end{bmatrix} \begin{bmatrix} 1 & 0 \\ 0 & 1 \end{bmatrix}, \quad Q : \begin{bmatrix} 2 \\ -4 \end{bmatrix} \begin{bmatrix} 1 & 0 \\ 0 & 1 \end{bmatrix} \quad \text{and} \quad D : \begin{bmatrix} -3 \\ -6 \end{bmatrix} \begin{bmatrix} 1 & -2 \\ 0 & 1 \end{bmatrix},$$

so T is a source, Q is a saddle repelling in H_D direction and D is a sink in $\overline{\mathcal{V}}_{\mathrm{VIII}}$.

It is proven in appendix A.1 that there are exactly two more fixed points at infinity, $T_\infty = [\infty, -1]^{\mathrm{T}}$ and $Q_\infty = [\infty, 1]^{\mathrm{T}}$. The stability properties then follow directly from (7): First, $\Sigma_+' > 0$ in $\mathcal{V}_{\mathrm{VIII}}$. Second, for $H_D > 2$ (and thus at infinity), $H_D' \gtreqless 0$ for $\Sigma_+ \lesseqgtr 0$. Hence T_∞ and Q_∞ play the role of saddles for the flow in $\overline{\mathcal{V}}_{\mathrm{VIII}}$ given in figure 4.

To interpret this as flow in $\overline{\mathcal{V}}^{\mathcal{Y}}_{\mathrm{VIII}}$, note that the fixed point T in $\overline{\mathcal{V}}_{\mathrm{VIII}}$ corresponds to the closure of the line $T_\flat \to T_\sharp$ in $\overline{\mathcal{V}}^{\mathcal{Y}}_{\mathrm{VIII}}$. Since $T_\flat$ and $T_\sharp$ turn out to act as a source and a saddle in $\overline{\mathcal{V}}^{\mathcal{Y}}_{\mathrm{VIII}}$ in all cases respectively, cf. figures 5 to 17, the orbits in $\mathcal{V}^{\mathcal{Y}}_{\mathrm{VIII}}$ have the form $T_\flat \to D$.

3.2. Analysis in $\overline{\mathcal{B}}_{\mathrm{III}}$.

The dynamical system in $\overline{\mathcal{B}}_{\mathrm{III}}$ is obtained from (2) by setting $M_1 = 0$ ($\Leftrightarrow s = 0$) and using (1):

$$\begin{bmatrix} H_D \\ \Sigma_+ \end{bmatrix}' = \begin{bmatrix} -(1 - H_D^2)\left(2 - \frac{3}{2}(1-w)(1-\Sigma_+^2) - H_D\Sigma_+\right) \\ -(1-\Sigma_+^2)\left((1-H_D^2) + \frac{3}{2}(1-w)(H_D\Sigma_+ + \beta)\right) \end{bmatrix} =: f(H_D, \Sigma_+) \tag{8}$$

[5]Here and henceforth the notation follows the pattern $P : \begin{bmatrix} \lambda_1 \\ \lambda_2 \end{bmatrix} [v_1, v_2]$ where λ_i and v_i denote the i^{th} eigenvalue and eigenvector of the linearisation of the dynamical system at P.

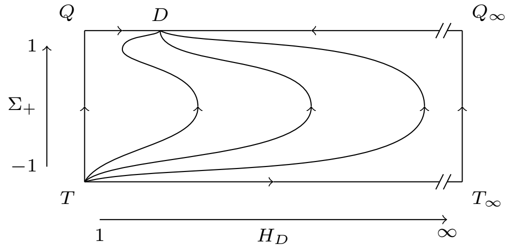

FIGURE 4. The flow in $\overline{\mathcal{V}}_{\mathrm{VIII}}$.

This system has at least three and at most five fixed points in $\overline{\mathcal{B}}_{\mathrm{III}}$ depending on $(w,\beta)\in\mathbb{P}$, namely

$$T_\flat := \begin{bmatrix}1\\-1\end{bmatrix}, Q_\flat := \begin{bmatrix}1\\1\end{bmatrix}, D = \begin{bmatrix}2\\1\end{bmatrix}, R_\flat := \begin{bmatrix}1\\-\beta\end{bmatrix} \text{ and } P := \begin{bmatrix}\frac{2+3\beta(1-w)}{\sqrt{(1-3w)^2+6\beta(1-w)}}\\ \frac{1+3w}{\sqrt{(1-3w)^2+6\beta(1-w)}}\end{bmatrix}.$$

Clearly $R_\flat$ is a fixed point in $\overline{\mathcal{B}}_{\mathrm{III}}$ (and different from $T_\flat$, $Q_\flat$) iff $\beta\in(-1,1)$. The conditions $H_D|_P>1$ and $\Sigma_+|_P<1$ entail that P is in $\mathcal{B}_{\mathrm{III}}$ iff $\beta>\beta_\flat(w):=\frac{2w}{1-w}$ and $(w,\beta)\notin\overline{\mathbb{P}}_\supset$, where $\mathbb{P}_\supset$ refers to the small $\supset$-shaped subset of $\mathbb{P}$ bounded by $\beta_\pm(w):=\frac{-1\pm\sqrt{-3+(1-3w)^2}}{3(1-w)}$; cf. figure 3. Under these conditions the square root in the coordinates of P is automatically real and $\Sigma_+|_P>0$.

The eigenvectors and eigenvalues of the linearisation $\mathrm{D}f(H_D,\Sigma_+)$ at $T_\flat,Q_\flat,D$ and $R_\flat$ determine their local stability properties. One finds

$$T_\flat:\begin{bmatrix}6\\3(1-w)(1-\beta)\end{bmatrix}\begin{bmatrix}1&0\\0&1\end{bmatrix},\qquad D:\begin{bmatrix}-3\\3\beta(1-w)-6w\end{bmatrix}\begin{bmatrix}1&\frac{1-3w}{1-2w+\beta(1-w)}\\0&1\end{bmatrix},$$

$$Q_\flat:\begin{bmatrix}2\\3(1-w)(1+\beta)\end{bmatrix}\begin{bmatrix}1&0\\0&1\end{bmatrix},\qquad R_\flat:\begin{bmatrix}3\beta^2(1-w)+1+3w+2\beta\\-\frac{3}{2}(1-w)(1-\beta^2)\end{bmatrix}\begin{bmatrix}\frac{3\beta^2(1-w)+5+3w+4\beta}{(1-\beta^2)(3\beta(1-w)+4)}&0\\1&1\end{bmatrix}.$$

Therefore, in $\overline{\mathcal{B}}_{\mathrm{III}}$, $T_\flat$ is a source for $\beta<1$ and a saddle repelling in H_D direction for $\beta>1$, $Q_\flat$ is a saddle repelling in H_D direction for $\beta<-1$ and a source for $\beta>-1$, D is a sink for $\beta<\beta_\flat(w)$ and a saddle attracting in H_D direction for $\beta>\beta_\flat(w)$ and $R_\flat$ is a sink $\forall(w,\beta)\in\mathbb{P}_\supset$ and a saddle attracting in Σ_+ direction $\forall(w,-1<\beta<1)\in\mathbb{P}\backslash\overline{\mathbb{P}}_\supset$.

The eigenvalues $\lambda_\pm$ of $\mathrm{D}f|_P$ are given in terms of trace and determinant by

$$2\lambda_\pm = \operatorname{tr}\mathrm{D}f|_P \pm\sqrt{(\operatorname{tr}\mathrm{D}f|_P)^2-4\det\mathrm{D}f|_P}, \tag{9}$$

where

$$\det\mathrm{D}f|_P=\frac{9(1-w)\big(3\beta^2(1-w)+1+3w+2\beta\big)\big(\beta(1-w)-2w\big)}{(1-3w)^2+6\beta(1-w)}, \tag{10}$$

$$\operatorname{tr}\mathrm{D}f|_P=-\frac{3(1-w)(1+2\beta)}{\sqrt{(1-3w)^2+6\beta(1-w)}}, \tag{11}$$

which are real whenever P exists in $\mathcal{B}_{\mathrm{III}}$ because the square root in (11) appears in the coordinates of P as well. Further, $\operatorname{tr}\mathrm{D}f|_P<0$ and $\det\mathrm{D}f|_P>0$ whenever P is in $\mathcal{B}_{\mathrm{III}}$.[6] Hence the real part of (9) is always negative, whether the eigenvalues are real or complex, so P is a sink in $\mathcal{B}_{\mathrm{III}}$ whenever present. The eigenvalues are real for $\beta\in(\beta_\flat(w),\beta^*_\flat(w)]$; cf. figure 3.

[6]To see the first inequality, note from figure 3 that $\beta>-\frac{1}{2}$ when P is in $\mathcal{B}_{\mathrm{III}}$. To see the second inequality, note that setting the middle and last factor in the numerator of (10) to zero corresponds to the bifurcation line $\beta_\pm(w)$ and $\beta_\flat(w)$, respectively.

In order to perform the analysis of the flow in the full state space $\mathcal{X}_{\text{VIII}}$ in section 3.5, it is also necessary to know the local stability of P in the direction of M_1: From (2) one has $(\ln M_1)'|_P = -3\Sigma_+|_P$, which is negative so that P is attracting in the direction of M_1. This implies that P is a local sink in $\overline{\mathcal{X}}_{\text{VIII}}$.

It is shown in appendix A.1 that there are exactly two more fixed points at infinity, $T_\infty = [\infty, -1]^{\text{T}}$ and $Q_\infty = [\infty, 1]^{\text{T}}$. Their stability properties then follow straightforwardly from (8): For H_D sufficiently large, $f(H_D, \Sigma_+) \approx [-H_D^3\Sigma_+, H_D^2(1-\Sigma_+^2)]^{\text{T}}$. Hence, $\Sigma_+' > 0$ and $H_D' \gtreqless 0$ for $\Sigma_+ \lesseqgtr 0$, which implies that T_∞ and Q_∞ play the role of saddles for the flow in $\overline{\mathcal{B}}_{\text{III}}$.

For the cases where P does not exist in $\mathcal{B}_{\text{III}}$, the information suffices to draw the corresponding qualitative flow diagrams. When P exists in $\mathcal{B}_{\text{III}}$, periodic orbits encircling this fixed point could in principle be present. However numeric investigations strongly suggest that this is not the case. In any case, the main results of this paper are not affected by this open question; cf. section 4.

The resulting qualitative dynamics in $\overline{\mathcal{B}}_{\text{III}}$ in dependence of $(w, \beta) \in \mathbb{P}$ is depicted in figures 5 to 17 as flows in $\overline{\mathcal{B}}_{\text{III}}^{\mathcal{Y}}$ together with the flows in $\overline{\mathcal{S}}_\sharp^{\mathcal{Y}}$ and $\overline{\mathcal{X}}_{\text{I}}$. The latter two subsets will be discussed next.

3.3. **Analysis in $\overline{\mathcal{S}}_\sharp$.** $\overline{\mathcal{S}}_\sharp$ is the common boundary of the state spaces $\mathcal{X}_{\text{VIII}}$ and $\mathcal{X}_{\text{IX}}$ of LRS types VIII and IX. It has been analysed in detail in [3, section 10.1]. The bifurcation lines $\beta = \pm 2$, $\beta_\sharp(w)$ and $\beta_\sharp^*(w)$ result from this analysis. The results are depicted in section 4 as flows in $\overline{\mathcal{S}}_\sharp^{\mathcal{Y}}$ together with the flows in $\overline{\mathcal{B}}_{\text{III}}^{\mathcal{Y}}$ and $\overline{\mathcal{X}}_{\text{I}}$.

3.4. **Analysis in $\overline{\mathcal{X}}_{\text{I}}$.** The flow in $\overline{\mathcal{X}}_{\text{I}}$ has been analysed in detail in [3, section 10.2]. The only new bifurcation line in figure 3 resulting from this analysis is $\beta = 0$ which corresponds to the local stability properties of the Friedmann point F. However the qualitative dynamics in $\overline{\mathcal{X}}_{\text{I}}$ is also associated with the bifurcation lines $\beta = \pm 1$ and $\beta = \pm 2$. The results are depicted in section 4 together with the flows in $\overline{\mathcal{B}}_{\text{III}}^{\mathcal{Y}}$ and $\overline{\mathcal{S}}_\sharp^{\mathcal{Y}}$.

3.5. **Analysis in $\overline{\mathcal{X}}_{\text{VIII}}$ and $\overline{\mathcal{S}}_\infty$.** The full system (2) does not have any fixed points in $\mathcal{X}_{\text{VIII}}$. Furthermore, as shown in appendix A.2 there are only the already know fixed points $T_\infty = [\infty, -1, 0]^{\text{T}}$ and $Q_\infty = [\infty, 1, 0]^{\text{T}}$ at infinity. Their stability properties then follow straightforwardly from (2): For H_D sufficiently large, $\text{rhs}(2) \approx [-H_D^3\Sigma_+, H_D^2(1-\Sigma_+^2), -H_D^2\Sigma_+ M_1]^{\text{T}}$. Hence $\Sigma_+' > 0$, $H_D' \gtreqless 0$ for $\Sigma_+ \lesseqgtr 0$ and $M_1' \gtreqless 0$ for $\Sigma_+ \lesseqgtr 0$, which implies that T_∞ and Q_∞ play the role of saddles for the flow in $\overline{\mathcal{X}}_{\text{VIII}}$. Viewing infinity as the boundary $\overline{\mathcal{S}}_\infty$ in a compactified version of the state space, T_∞ is a source and Q_∞ is a sink in $\overline{\mathcal{S}}_\infty$, hence all orbits in $\overline{\mathcal{S}}_\infty$ are of the form $T_\infty \to Q_\infty$.

An important consequence is that there is no orbit in $\mathcal{X}_{\text{VIII}}$ that emanates from or escapes to infinity. Hence each orbit in $\mathcal{X}_{\text{VIII}}$ lies in a compact subset. The following lemma concludes this section. It will also be used to localise the α- and ω-limit sets [6, p 99 Def 4.12] in the next section; cf. [6, p 91 Def 4.7] for the term 'invariant set':

Lemma 1. *Let γ be an orbit in $\mathcal{Y}_{\text{VIII}}$. Then both, $\alpha(\gamma)$ and $\omega(\gamma)$, is a non-empty, compact and connected invariant subset of $\overline{\mathcal{Y}}_{\text{VIII}}$. Furthermore, $\alpha(\gamma) \subseteq \overline{\mathcal{S}}_\sharp^{\mathcal{Y}} \cup \overline{\mathcal{X}}_{\text{I}}$ and $\omega(\gamma) \subseteq \overline{\mathcal{B}}_{\text{III}}^{\mathcal{Y}} \cup \overline{\mathcal{X}}_{\text{I}}$.*

Proof. First, since each orbit in $\mathcal{X}_{\text{VIII}}$ lies in a compact subset, so does by (4) each orbit in $\mathcal{Y}_{\text{VIII}}$. The first statement of the lemma then follows from [6, p 99 Thm 4.9].

Second, consider the function $Z_5 : \mathcal{X}_{\mathrm{VIII}} \cup \mathcal{V}_{\mathrm{VIII}} \to \mathbb{R}$ given by

$$Z_5 := \frac{H_D M_1^{\frac{1}{3}}}{(H_D^2 - 1)^{\frac{2}{3}}} > 0 \quad \text{with} \quad Z_5' = -\frac{4\Sigma_+ + (1+3w)\Omega}{2H_D} Z_5 \leq 0.$$

One can check that $Z_5''|_{\Sigma_+=\Omega=0} = 0$ and $Z_5'''|_{\Sigma_+=\Omega=0} < 0$ in $\mathcal{X}_{\mathrm{VIII}}$, which means that Z_5 is strictly monotonically decreasing along the flow in $\mathcal{X}_{\mathrm{VIII}}$. Hence the monotonicity principle [6, p 103 Thm 4.12] implies that the limit sets lie in $\overline{\mathcal{B}}_{\mathrm{III}} \cup \overline{\mathcal{S}}_\sharp$. Moreover, since $Z_5 \to 0 = \inf(Z_5)$ when one approaches $\mathcal{B}_{\mathrm{III}}$ and $Z_5 \to \infty = \sup(Z_5)$ when one approaches $\mathcal{S}_\sharp$, the monotonicity principle implies $\alpha(\tilde{\gamma}) \subseteq \overline{\mathcal{S}}_\sharp$ and $\omega(\tilde{\gamma}) \subseteq \overline{\mathcal{B}}_{\mathrm{III}}$ for all orbits $\tilde{\gamma}$ in $\mathcal{X}_{\mathrm{VIII}}$. In the context of $\mathcal{Y}_{\mathrm{VIII}}$ this means that $\alpha(\gamma) \subseteq \overline{\mathcal{S}}_\sharp^{\mathcal{Y}} \cup \overline{\mathcal{X}}_{\mathrm{I}}$ and $\omega(\gamma) \subseteq \overline{\mathcal{B}}_{\mathrm{III}}^{\mathcal{Y}} \cup \overline{\mathcal{X}}_{\mathrm{I}}$; cf. (5). □

4. Results and discussion

Finally all information obtained in section 3 can be collected to identify the α- and ω-limit sets of generic orbits $\gamma \in \mathcal{Y}_{\mathrm{VIII}}$, and hence the past and future asymptotic dynamics of generic LRS Bianchi type VIII cosmologies, for all qualitatively different anisotropic matter cases:

4.1. **Identification of the limit sets.** Figure 3 shows that there are thirteen qualitatively different cases.[7] These cases are listed in figures 5 to 17, which show, for each case, a plot of the bifurcation diagram where the corresponding subset of $\mathbb{P}$ is shaded and a representative flow diagram in the set $\overline{\mathcal{S}}_\sharp^{\mathcal{Y}} \cup \overline{\mathcal{X}}_{\mathrm{I}} \cup \overline{\mathcal{B}}_{\mathrm{III}}^{\mathcal{Y}}$, on which the limit sets lie by lemma 1. Solid (dashed) lines represent generic (non-generic) orbits in the respective boundary subset. A filled (empty) circle on a fixed point indicates that it attracts (repels) orbits in the respective orthogonal direction.[8] Heteroclinic cycles and networks are represented by thick lines. The axes with two labels emphasise the diffeomorphisms (6) and the bijection between s and θ; cf. section 2.4.

By lemma 1, the limit sets are non-empty, compact and connected invariant subsets of $\overline{\mathcal{Y}}_{\mathrm{VIII}}^{\mathcal{Y}}$. This leaves fixed points, heteroclinic cycles and heteroclinic networks as candidates for the limit sets in figures 5 to 17.

A single fixed point is an (α-) ω-limit set of generic orbits $\gamma \in \mathcal{Y}_{\mathrm{VIII}}$ iff it (repels) attracts orbits from a three dimensional neighbourhood in $\mathcal{Y}_{\mathrm{VIII}}$; e.g. a (source) sink. These can easily be identified from the figures. In the cases of figures 9 to 16, fixed points are the only possible generic limit sets. Furthermore, these cases exhibit just one source and sink respectively, which implies that these are the past/future attractors [6, p 100 Def 4.13].

Figures 5 to 8 and 17 show a heteroclinic cycle or network each, and hence additional candidates for limit sets. In figures 7 and 8 the cycle is the past attractor since there is no other candidate for a generic α-limit set in $\overline{\mathcal{S}}_\sharp^{\mathcal{Y}} \cup \overline{\mathcal{X}}_{\mathrm{I}}$, and as proven in section 3.5 $\alpha(\gamma)$ is non-empty. Note that since the cycle is not in $\overline{\mathcal{B}}_{\mathrm{III}}^{\mathcal{Y}} \cup \overline{\mathcal{X}}_{\mathrm{I}}$ it cannot be an ω-limit set. The same line of arguments shows that in figures 5 and 6 the past attractor is a subset of the heteroclinic network.

In figure 17, the heteroclinic network could be an α-limit set in addition to $T_\flat$. Analogously, in figures 5 and 6, the heteroclinic cycle $\partial\mathcal{X}_{\mathrm{I}}$ could be an ω-limit set in addition to D and P, respectively. The nontrivial task of directly tackling the stability properties of these structures is omitted here. They are however taken

[7] The bifurcation lines $\beta_\flat^*(w)$ and $\beta_\sharp^*(w)$ only specify if the fixed points $C_\sharp$ and P are local stable nodes or foci in $\mathcal{S}_\sharp^{\mathcal{Y}}$ and $\mathcal{B}_{\mathrm{III}}^{\mathcal{Y}}$ respectively, which is irrelevant for identifying the limit sets.

[8] The colour coding of T_∞ and Q_∞ makes only sense in the context of $\mathcal{X}_{\mathrm{VIII}}$. The fixed points in $\partial\mathcal{X}_{\mathrm{I}}$ are not colour coded since the orthogonal directions are represented in the figures.

Fixed points	corresponding solution	type	vacuum
$T_\flat, T_\sharp$	Taub Kasner	I	✓
$Q_\flat, Q_\sharp$	non-flat LRS Kasner	I	✓
$R_\flat, R_\sharp$	a type I anisotropic matter solution	I	
F	flat Friedmann	I	
$C_\sharp$	generalisation of Collins-Stewart	II	
P	generalisation of Collins (VI_{-1})	III	
D	type III form of flat spacetime	III	✓

TABLE 1. The exact solutions corresponding to the fixed points.

into account as further candidates for generic limit sets in these three cases. Note that figure 17 is the only one of these three cases where the energy conditions can be satisfied; cf. section 2.1 and figure 3.

4.2. **The main results.** Finally one arrives at the main theorem and its corollaries:

Theorem 1. *The α- and ω-limit sets of generic orbits $\gamma \in \mathcal{Y}_{\mathrm{VIII}}$ of the dynamical system (2) with parameters $(w,\beta) \in \mathbb{P}$, is given as stated in the captions of figures 5 to 17. These describe the past and future asymptotic dynamics of LRS Bianchi type VIII cosmologies with anisotropic matter of the family defined in section 2.1.*

Proof. Cf. section 4.1. □

The exact solutions corresponding to the fixed points are summarised in table 1. These have been given in [3, appendix A] for all fixed points but D. For D, one just needs to insert the coordinates into [3, Eq 99]. The corresponding isotropic cases to these solutions can be found in [6, section 9.1].

Vacuum and perfect fluid cases. *LRS Bianchi type VIII vacuum solutions are past asymptotic to $T_\flat$ and future asymptotic to D.*

Generic LRS Bianchi type VIII solutions with a non-tilted perfect fluid where $p = w\rho$ and $w \in \left(-\frac{1}{3}, 1\right)$ are past asymptotic to $T_\flat$, future asymptotic to P for $w \in \left(-\frac{1}{3}, 0\right)$ and to D for $w \in [0,1)$.

The vacuum part follows from section 3.1; cf. figure 4. For the perfect fluid cases, recall from section 2.1 that they correspond to the line $\beta = 0$ in $\mathbb{P}$. They are therefore contained in theorem 1 as special cases.[9] The only bifurcation line intersecting $\beta = 0$ is $\beta_\flat(w)$ at $w = 0$ which yields the two qualitatively different perfect fluid cases, see figures 12 and 13, respectively. The statement on the future asymptotics for $w \in \left(-\frac{1}{3}, 0\right)$ might fill a little gap in the literature. The other results are known: The past asymptotics has been given in [7, table 4 and figure 4], the future asymptotics for vacuum in [8, Prop 8.1] and the future asymptotics for perfect fluids with $w \in [0,1)$ in [9, Thm 3.1].

Comparison with the cases of theorem 1 shows that the dynamics with anisotropic matter differs from the vacuum and perfect fluid cases in figures 5 to 8, 14 and perhaps 17. The strongest implications of this represent the main results of this paper stated in the following corollaries:

Corollary 1 (**past asymptotics**). *The past asymptotic dynamics of generic LRS Bianchi type VIII cosmologies with anisotropic matter can differ significantly from that of the vacuum and perfect fluid cases. In particular, the approach to the initial singularity is oscillatory in the cases depicted in figures 5 to 8 and perhaps 17.*

[9]The fact that $\beta = 0$ is itself a bifurcation line, which is related to the stability of the Friedmann point, is not relevant for the asymptotic dynamics.

Corollary 2 (**future asymptotics**). *The future asymptotic dynamics of generic LRS Bianchi type VIII cosmologies with anisotropic matter can differ significantly from that of the vacuum and perfect fluid cases. Note in particular the cases of figures 14 and perhaps 5 and 6.*

For completeness it is necessary to elaborate on the remark at the end of section 3.2 concerning the possible occurrence of periodic orbits around P in $\mathcal{B}^{\mathcal{Y}}_{\mathrm{III}}$: Such orbits are not observed numerically. However, their occurrence could change certain details in theorem 1, adding further ω-limit candidates in the cases where P is in $\mathcal{B}^{\mathcal{Y}}_{\mathrm{III}}$. On the other hand, corollary 1 would be completely untouched and corollary 2 even strengthened by the occurrence of such periodic orbits.

4.3. **Physical interpretation of the results.** An interesting observation is that there is a neighbourhood of the line $\beta = 0$ in $\mathbb{P}$ for which the corresponding asymptotic dynamics is identical to that of the perfect fluid cases. Hence the perfect fluid solutions are robust under small perturbations of a vanishing anisotropy parameter. For the past asymptotics to differ from that, β even needs to be so high that the dominant energy condition is only marginally satisfied.

The specialisation of the results to the cases for which the energy conditions are satisfied is obtained by restricting β to $\left[\max\left(-2, -\frac{1+w}{1-w}\right), 1\right]$; cf. section 2.1. This corresponds to the shaded region in figure 3, and thus rules out the cases of figures 5 and 6. All other cases contain values (w, β) for which the energy conditions are satisfied.

However, it should be pointed out that the cases represented by figures 7 and 8 only satisfy the energy conditions for $\beta = 1$, and the case of figure 17 only for $w \geq \frac{1}{3}$ and $\beta = -2$, i.e. for (w, β) in one-dimensional subsets of $\mathbb{P}$ for which the dominant energy condition is only marginally satisfied. Consequently, in these cases the energy flow is necessarily lightlike close to the singularity. A special example is given by collisionless (Vlasov) matter with massless particles, which as shown in [3, section 12.1] falls into the class of matter models with $(w, \beta) = \left(\frac{1}{3}, 1\right)$.

In any case, the statements of corollaries 1 and 2 remain true under the restriction to matter satisfying the energy conditions.

This concludes the main results on the anisotropic matter analysis. Section 5 is concerned with an extension of the present formalism to treat LRS type VIII dynamics with Vlasov matter with massive particles, which does not a priori fit into the anisotropic matter family considered so far.

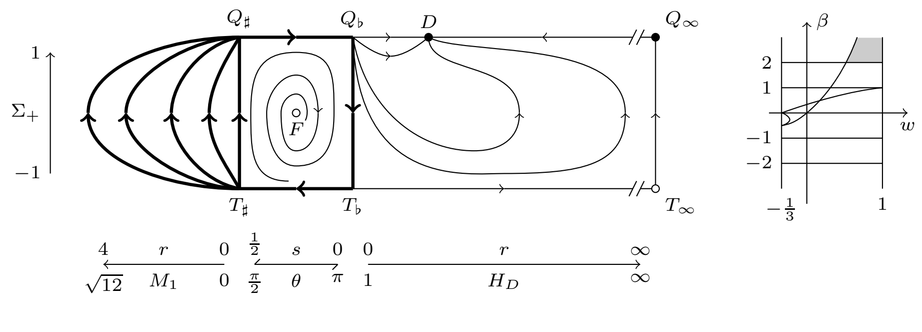

FIGURE 5. $\alpha(\gamma) \subseteq \text{network}(T_\flat, T_\sharp, Q_\sharp, Q_\flat)$. $\omega(\gamma) = D$, possibly $\partial\mathcal{X}_{\mathrm{I}}$.

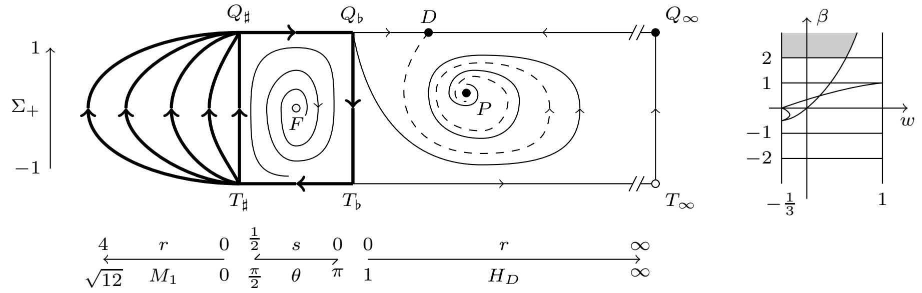

FIGURE 6. $\alpha(\gamma) \subseteq \text{network}(T_\flat, T_\sharp, Q_\sharp, Q_\flat)$. $\omega(\gamma) = D$, possibly $\partial\mathcal{X}_{\mathrm{I}}$.

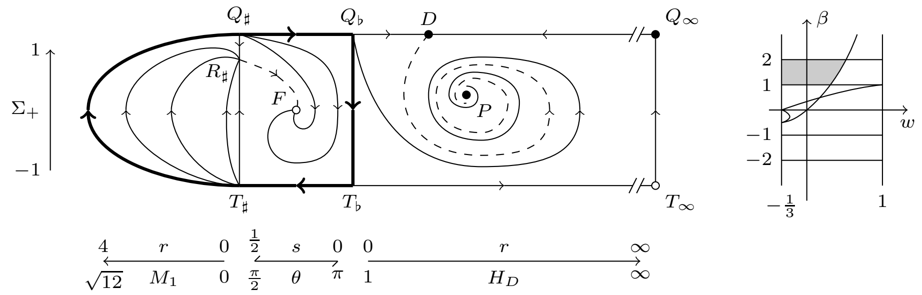

FIGURE 7. $\alpha(\gamma) = \text{cycle}(T_\flat, T_\sharp, Q_\sharp, Q_\flat)$. $\omega(\gamma) = P$.

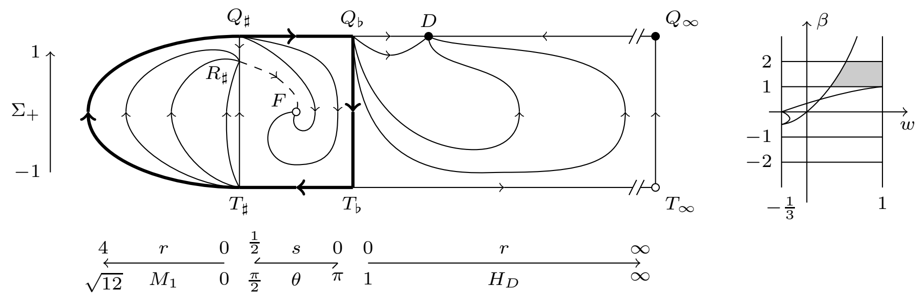

FIGURE 8. $\alpha(\gamma) = \text{cycle}(T_\flat, T_\sharp, Q_\sharp, Q_\flat)$. $\omega(\gamma) = D$.

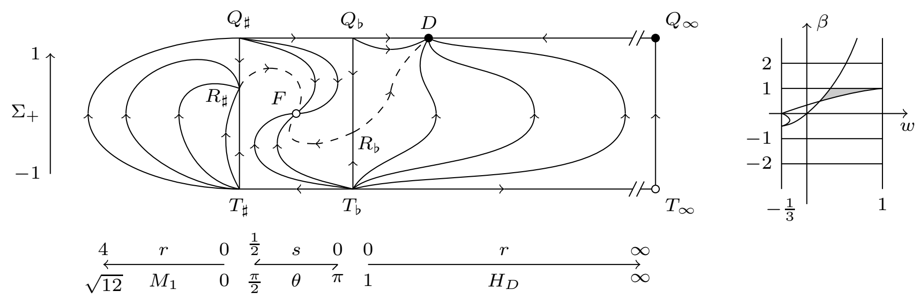

FIGURE 9. $\alpha(\gamma) = T_\flat$. $\omega(\gamma) = D$.

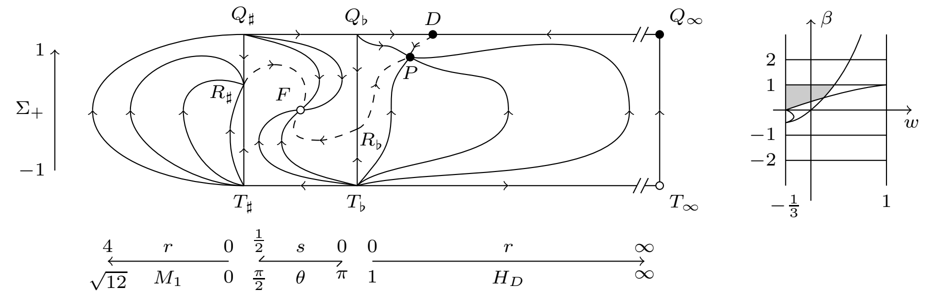

FIGURE 10. $\alpha(\gamma) = T_\flat$. $\omega(\gamma) = P$.

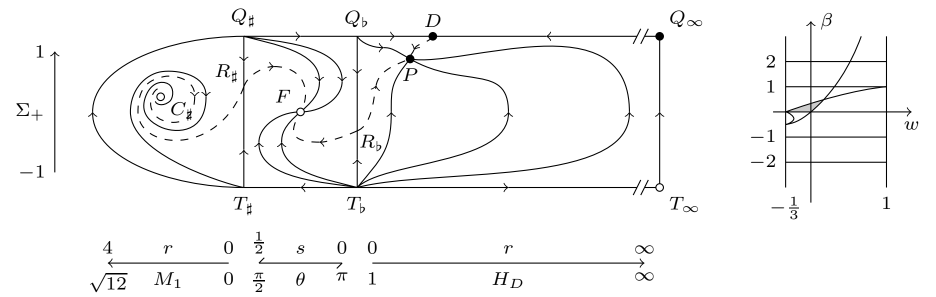

FIGURE 11. $\alpha(\gamma) = T_\flat$. $\omega(\gamma) = P$.

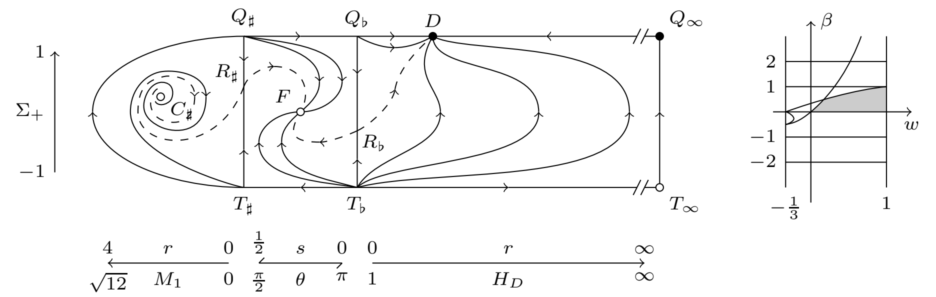

FIGURE 12. $\alpha(\gamma) = T_\flat$. $\omega(\gamma) = D$.

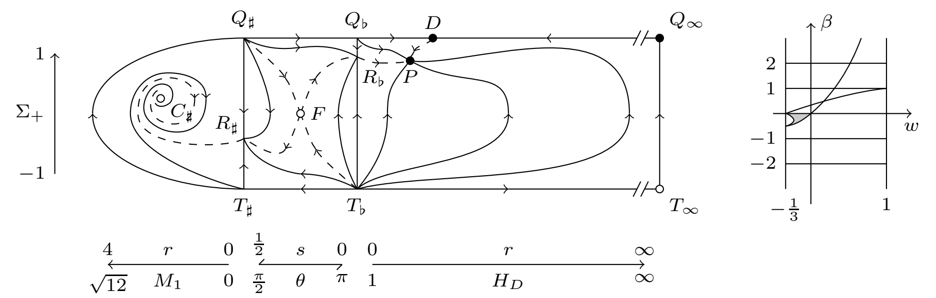

FIGURE 13. $\alpha(\gamma) = T_\flat$. $\omega(\gamma) = P$.

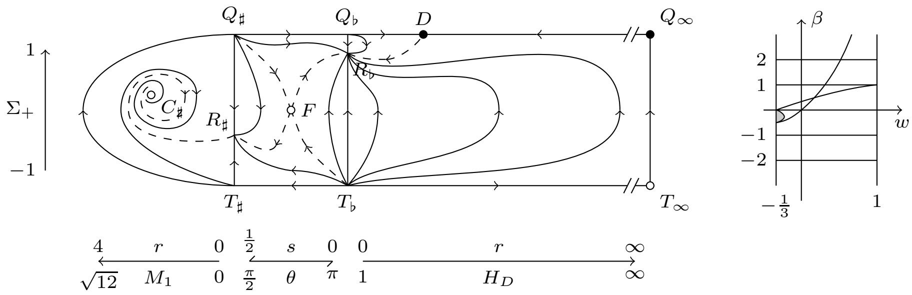

FIGURE 14. $\alpha(\gamma) = T_\flat$. $\omega(\gamma) = R_\flat$.

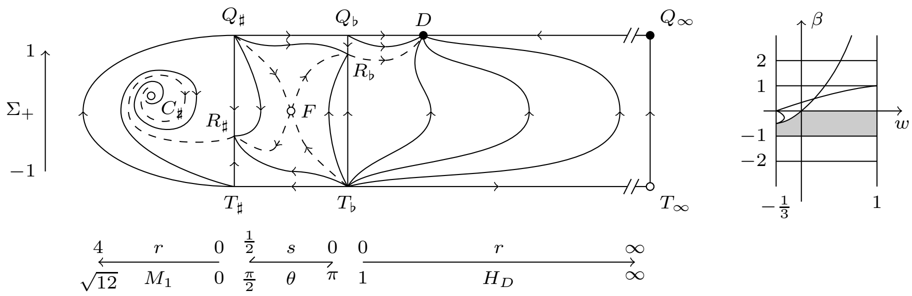

FIGURE 15. $\alpha(\gamma) = T_\flat$. $\omega(\gamma) = D$.

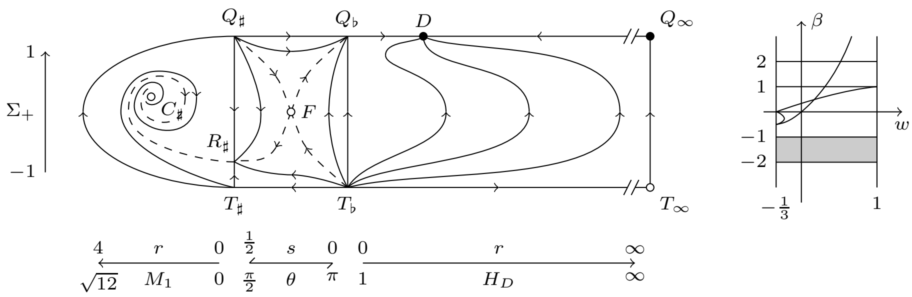

FIGURE 16. $\alpha(\gamma) = T_\flat$. $\omega(\gamma) = D$.

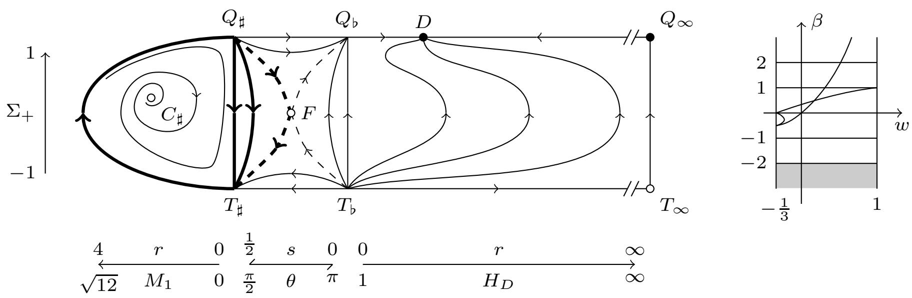

FIGURE 17. $\alpha(\gamma) = T_\flat$, possibly network$(T_\sharp, Q_\sharp, F)$. $\omega(\gamma) = D$.

5. Extension of the formalism to treat Vlasov matter dynamics with massive particles

It was stated in section 4.3 that Vlasov matter with massless particles falls into the class of matter models described in section 2.1 with parameters $(w, \beta) = (\frac{1}{3}, 1)$. This is shown in [3, section 12.1]. However, as stated there, for Vlasov matter with massive particles the relation $p = w\rho$ is non-linear. In [4], Calogero and Heinzle extended their formalism to treat Vlasov matter dynamics with massive particles in the case of LRS type IX. Since types VIII and IX are analogous in this formulation, and in particular share the same evolution equations, this extension of the formalism can be adopted to LRS type VIII without difficulties:

Following [4, section 3], the dynamical system representing the LRS type VIII Einstein-Vlasov system is given by the system (2) and the additional equation

$$l' = 2H_D l(1 - l). \tag{12}$$

The additional variable $l := \frac{(\det g)^{1/3}}{1+(\det g)^{1/3}} \in (0, 1)$ corresponds to a length scale of the spatial metric. The rescaled principal pressures are functions of l and s. Their full expressions are given in [4, Eq 13] from which it follows that

$$(w, \beta)|_{l=0} = \left(\tfrac{1}{3}, 1\right) \qquad \text{and} \qquad (w, \beta)|_{l=1} = (0, 0). \tag{13}$$

The LRS type VIII state space for Vlasov matter dynamics is given by $\mathcal{X}_{\mathrm{VIII}} \times (0, 1)$.

The dynamical system can be analysed as follows: By (12), l is strictly monotonically increasing along orbits in $\overline{\mathcal{X}}_{\mathrm{VIII}} \times (0, 1)$. The monotonicity principle thus implies that $\alpha(\gamma) \subseteq \overline{\mathcal{X}}_{\mathrm{VIII}} \times \{0\}$ and $\omega(\gamma) \subseteq \overline{\mathcal{X}}_{\mathrm{VIII}} \times \{1\}$.[10] Hence, the search for the limit sets can be restricted to these boundary subsets:

From (13), the flow in $\overline{\mathcal{X}}_{\mathrm{VIII}} \times \{0\}$ is equivalent to the flow for anisotropic matter with parameters $(\frac{1}{3}, 1)$; cf. figure 8. Hence the cycle$(T_\flat, T_\sharp, Q_\sharp, Q_\flat)$ is the past attractor of the flow in $\mathcal{X}_{\mathrm{VIII}} \times (0, 1)$, since this cycle is the only candidate for an α-limit set for generic orbits. Also from (13), the flow in $\overline{\mathcal{X}}_{\mathrm{VIII}} \times \{1\}$ is equivalent to the flow for anisotropic matter with parameters $(0, 0)$, i.e. to that for dust; cf. figure 12. Hence D is the future attractor of the flow in $\mathcal{X}_{\mathrm{VIII}} \times (0, 1)$, since this fixed point is the only candidate for an ω-limit set for generic orbits.

$l = 0$ corresponds to Vlasov dynamics with massless particles; cf. [4, section 3]. Hence the result states that Vlasov matter with massive particles behaves like Vlasov matter with massless particles asymptotically to the past, and like dust asymptotically to the future.

Appendix A. Fixed points at infinity

To find the fixed points of (2), (7) and (8) at infinity, a method presented in [10, 3.10] is adopted in a slightly modified way:

A.1. In two dimensions.

Consider a two dimensional system

$$\begin{bmatrix} H_D \\ \Sigma_+ \end{bmatrix}' = \begin{bmatrix} P(H_D, \Sigma_+) \\ Q(H_D, \Sigma_+) \end{bmatrix}$$

where P and Q are polynomials of degree n and m in H_D respectively, satisfying $n \leq m + 1$. One can write this system as

$$Q(H_D, \Sigma_+)\mathrm{d}H_D - P(H_D, \Sigma_+)\mathrm{d}\Sigma_+ = 0, \tag{14}$$

where however the information about the direction of the flow is lost. Next the H_D coordinate is formally compactified by projecting the state space onto the

[10] One can use the same arguments as in section 3.5 and appendix A for each $l = \text{const}$ hypersurface to prove that all orbits can be trapped in a compact subset of $\mathbb{R}^4$.

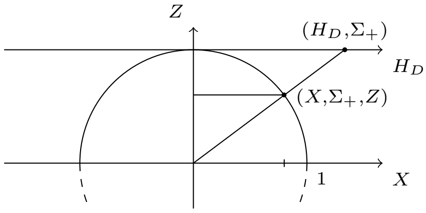

FIGURE 18. Projection onto the 'Poincaré cylinder'.

'Poincaré cylinder' as illustrated in figure 18. The corresponding coordinate transformation $(H_D, \Sigma_+) \to (X, \Sigma_+, Z) : X^2 + Z^2 = 1$ is given by $H_D = \frac{X}{Z}$. Applying this to (14) and multiplying by Z^{m+2} yields

$$Z^{m+1}Q(X/Z, \Sigma_+)\mathrm{d}X - Z^{m+2}P(X/Z, \Sigma_+)\mathrm{d}\Sigma_+ - XZ^m Q(X/Z, \Sigma_+)\mathrm{d}Z = 0, \tag{15}$$

which defines a flow on the 'Poincaré cylinder'; cf. [10, p 267]. Points at infinity in the original state space correspond to points on the 'equator' $X = 1, Z = 0$ on the 'Poincaré cylinder'. Furthermore, evaluating (15) with $X = 1, Z = 0$ gives the flow on the 'equator', which corresponds to the flow at infinity,

$$\big(Z^m Q(X/Z, \Sigma_+)\big)\big|_{X=1,Z=0}\mathrm{d}Z = 0. \tag{16}$$

Note that the first two terms of (15) vanish since they are at least proportional to Z. This is not true however for the third term of (15). From (16), for $(Z^m Q)|_{X=1,Z=0} \neq 0$ it follows that $\mathrm{d}Z = 0$, which corresponds to trajectories through a regular point on the 'equator', where the sign of $(Z^m Q)|_{X=1,Z=0}$ determines the flow direction. Fixed points on the 'equator' correspond to solutions of $(Z^m Q)|_{X=1,Z=0} = 0$; cf. [10, p 268 Thm 1]. Solving this equation for Q in the context of (7) and (8) yields $\Sigma_+ = \pm 1$ for the fixed points at infinity in $\mathcal{V}_{\mathrm{VIII}}$ and $\mathcal{B}_{\mathrm{III}}$ respectively, i.e. $T_\infty := [\infty, -1]^{\mathrm{T}}$ and $Q_\infty := [\infty, 1]^{\mathrm{T}}$.

A.2. **In three dimensions.** The generalisation to three or more dimensions is straightforward; cf. [10, p 277 ff]. Consider a three dimensional system

$$\begin{bmatrix} H_D \\ \Sigma_+ \\ M_1 \end{bmatrix}' = \begin{bmatrix} P(H_D, \Sigma_+, M_1) \\ Q(H_D, \Sigma_+, M_1) \\ R(H_D, \Sigma_+, M_1) \end{bmatrix}$$

where P, Q and R are polynomials of degree l, n and m in H_D respectively, satisfying $n + 1 \geq l \leq m + 1$. One can write this system as

$$\begin{aligned} Q(H_D, \Sigma_+, M_1)\mathrm{d}H_D - P(H_D, \Sigma_+, M_1)\mathrm{d}\Sigma_+ &= 0 \\ R(H_D, \Sigma_+, M_1)\mathrm{d}H_D - P(H_D, \Sigma_+, M_1)\mathrm{d}M_1 &= 0, \end{aligned} \tag{17}$$

where however the information about the direction of the flow is lost. Again the H_D coordinate is formally compactified by means of a projection on the 'Poincaré cylinder', i.e. by a coordinate transformation $(H_D, \Sigma_+, M_1) \to (X, \Sigma_+, M_1, Z) : X^2 + Z^2 = 1$ given by $H_D = \frac{X}{Z}$. Applying this to (17), multiplying by Z^{m+2} and Z^{n+2} respectively and evaluating the resulting expressions at the 'equator' $X = 1, Z = 0$ yields

$$\begin{aligned} \big(Z^m Q(X/Z, \Sigma_+, M_1)\big)\big|_{X=1,Z=0}\mathrm{d}Z &= 0 \\ \big(Z^n R(X/Z, \Sigma_+, M_1)\big)\big|_{X=1,Z=0}\mathrm{d}Z &= 0. \end{aligned}$$

Trajectories through a regular point on the 'equator' corresponds to $\mathrm{d}Z = 0$, where the flow direction is determined by the signs of $\big(Z^m Q(X/Z, \Sigma_+, M_1)\big)\big|_{X=1,Z=0}$ and $\big(Z^n R(X/Z, \Sigma_+, M_1)\big)\big|_{X=1,Z=0}$. Fixed points on the 'equator' correspond to

solutions of the system of equations $\{(Z^m Q)|_{X=1,Z=0} = 0, (Z^n R)|_{X=1,Z=0} = 0\}$. Solving this for Q and R in the context of (2) yields $\Sigma_+ = \pm 1, M_1 = 0$ for the fixed points at infinity in $\mathcal{X}_{\mathrm{VIII}}$, i.e. $T_\infty := [\infty, -1, 0]^{\mathrm{T}}$ and $Q_\infty := [\infty, 1, 0]^{\mathrm{T}}$.

Acknowledgements

First and foremost, I am grateful to J Mark Heinzle who suggested this topic to me and provided guidance during the whole project. I am also thankful for the discussions I had with S Calogero and C Uggla during the workshop 'Dynamics of General Relativity' at the Erwin Schrödinger Institute for Mathematical Physics in Vienna in summer 2011.

References

[1] Heinzle JM, Uggla C, Röhr N: The cosmological billiard attractor; *Advances in Theoretical and Mathematical Physics (Volume 13, Number 2, Pages 293–407)*, International Press (2009).
Preprint: arXiv:gr-qc/0702141v1
Cited on page 1

[2] Calogero S, Heinzle JM: Dynamics of Bianchi type I Solutions of the Einstein Equations with Anisotropic Matter; *Annales Henri Poincaré (Volume 10, Number 2, Pages 225–274)*, Springer-Verlag/Birkhäuser Science (2009).
Preprint: arXiv:0809.1008v2 [qr-qc]
Cited on page 1

[3] Calogero S, Heinzle JM: Bianchi Cosmologies with Anisotropic Matter: Locally Rotationally Symmetric Models; *Physica D: Nonlinear Phenomena (Volume 240, Issue 7, Pages 636–669)*, Elservier (2010).
Preprint: arXiv:0911.0667v1 [gr-qc].
Cited on pages 1, 2, 3, 4, 5, 8, 10, 11, 15

[4] Calogero S, Heinzle JM: Oscillations toward the Singularity of Locally Rotationally Symmetric Bianchi Type IX Cosmological Models with Vlasov Matter; *SIAM Journal on Applied Dynamical Systems (Volume 9, Issue 4, Pages 1244–1262)*, Society for Industrial and Applied Mathematics (2010).
Preprint: arXiv:1011.3982v1 [gr-qc]
Cited on pages 2, 15

[5] Wald RM: General Relativity, The University of Chicago Press (1984).
Cited on page 3

[6] Wainwright J, Ellis GFR (editors): Dynamical Systems in Cosmology, Cambridge University Press (1997).
Cited on pages 3, 8, 9, 10

[7] Wainwright J, Hsu L: A dynamical systems approach to Bianchi cosmologies: orthogonal models of class A; *Classical and Quantum Gravity (Volume 6, Number 10, Pages 1409–1431)*, Institute of Physics Publishing (1989).
Cited on page 10

[8] Ringström H: The future asymptotics of Bianchi VIII vacuum solutions; *Classical and Quantum Gravity (Volume 18, Number 18, Pages 3791–3823)*, Institute of Physics Publishing (2001).
Preprint: arXiv:gr-qc/0103107v1
Cited on page 10

[9] Horwood JT, Hancock MJ, The D, Wainwright J: Late-time asymptotic dynamics of Bianchi VIII cosmologies; *Classical and Quantum Gravity (Volume 20, Number 9, Pages 1757–1777)*, Institute of Physics Publishing (2003).
Preprint: arXiv:gr-qc/0210031v2
Cited on page 10

[10] Perko L: Differential Equations and Dynamical Systems, second edition; *Texts in applied Mathematics 7*, Springer-Verlag (1996).
Cited on pages 15, 16

Gravitational Physics Group, Faculty of Physics, University of Vienna, Austria
E-mail address: Gernot.Heissel@Mac.com